



Insertional mutagenesis in a HER2-positive breast cancer model reveals ERAS as a driver of cancer and therapy resistance

Gerjon J. Ikkink¹ · Mandy Boer¹ · Elvira R. M. Bakker¹ · Annabel Vendel-Zwaagstra¹ · Chris Klijn² · Jelle ten Hoeve³ · Jos Jonkers² · Lodewyk F. Wessels³ · John Hilkens¹

Received: 6 April 2017 / Revised: 29 October 2017 / Accepted: 31 October 2017 / Published online: 12 January 2018
© The Author(s) 2018. This article is published with open access

Abstract

Personalized medicine for cancer patients requires a deep understanding of the underlying genetics that drive cancer and the subsequent identification of predictive biomarkers. To discover new genes and pathways contributing to oncogenesis and therapy resistance in HER2+ breast cancer, we performed Mouse Mammary Tumor Virus (MMTV)-induced insertional mutagenesis screens in *ErbB2/cNeu*-transgenic mouse models. The screens revealed 34 common integration sites (CIS) in mammary tumors of MMTV-infected mice, highlighting loci with multiple independent MMTV integrations in which potential oncogenes are activated, most of which had never been reported as MMTV CIS. The CIS most strongly associated with the *ErbB2*-transgenic genotype was the locus containing *Eras* (ES cell-expressed Ras), a constitutively active RAS-family GTPase. We show that upon expression, *Eras* acts as a potent oncogenic driver through hyperactivation of the PI3K/AKT pathway, in contrast to other RAS proteins that signal primarily via the MAPK/ERK pathway and require upstream activation or activating mutations to induce signaling. We additionally show that ERAS synergistically enhances HER2-induced tumorigenesis and, in this role, can functionally replace ERBB3/HER3 by acting as a more powerful activator of PI3K/AKT signaling. Although previously reported as pseudogene in humans, we observed ERAS RNA and protein expression in a substantial subset of human primary breast carcinomas. Importantly, we show that ERAS induces primary resistance to the widely used HER2-targeting drugs Trastuzumab (Herceptin) and Lapatinib (Tykerb/Tyverb) in vivo, and is involved in acquired resistance via selective upregulation during treatment in vitro, indicating that ERAS may serve as a novel clinical biomarker for PI3K/AKT pathway hyperactivation and HER2-targeted therapy resistance.

Introduction

HER2+ breast cancer is highly aggressive and afflicted patients have a poor clinical outcome [1]. Treatment with the humanized monoclonal antibody against ERBB2, Trastuzumab, or the small molecule kinase inhibitor

Lapatinib, typically combined with chemotherapy, significantly improves the clinical outcome [2, 3], but inherent and acquired resistance to both drugs are prevalent [4]. To study HER2+ breast cancer, various transgenic mouse strains have been raised as models for the human disease [5–8], in which mammary tumors stochastically arise that closely recapitulate the histopathological and molecular features of HER2+ human breast carcinomas [9, 10].

Insertional mutagenesis in mouse models is an effective method to discover novel genes involved in breast cancer development. We and others have previously identified a series of novel candidate cancer genes using MMTV-mediated insertional mutagenesis in mice [11–15]. MMTV causes a high incidence of murine mammary carcinomas by random insertion of its proviral DNA into the host DNA, which can activate adjacent proto-oncogenes [16–18]. The genomic localization of the proviral insertion can easily be determined using the technologies developed in our

Electronic supplementary material The online version of this article (<https://doi.org/10.1038/s41388-017-0031-0>) contains supplementary material, which is available to authorized users.

✉ John Hilkens
j.hilkens@nki.nl

¹ Division of Molecular Genetics, The Netherlands Cancer Institute, Amsterdam, The Netherlands

² Division of Molecular Pathology, The Netherlands Cancer Institute, Amsterdam, The Netherlands

³ Division of Molecular Carcinogenesis, The Netherlands Cancer Institute, Amsterdam, The Netherlands

laboratory [11, 14], thus allowing the identification of candidate oncogenes.

We performed high-throughput insertional mutagenesis screens in MMTV-infected *ErbB2*-transgenic mice to identify genes and pathways that collaborate with *ERBB2*-overexpression in mammary tumorigenesis. Combined results of a screen using the classical splinkerette PCR

method [11] and a screen using our Shear-Splink technology followed by deep sequencing [14, 19], revealed 34 common integration sites (CIS) associated with putative oncogenes, of which the majority has not previously been reported as an MMTV CIS.

We found the *Eras* gene as the most common MMTV-proviral target specific to *ErbB2*-induced mammary tumors.

Table 1 CISs found in the insertional mutagenesis screens in tumors from *MMTV-cNeu* mice

Locus	Chr.	Tumors with insertion (classical setup)	Tumors with insertion (Shear-Splink)	Known MMTV target	CIS in RTCGD (retrovirus)	CIS in RTCGD (transposon)
Wnt1/Wnt10b	15F1	16	14	Yes	28	—
Eras	XA1.1	8	11	Yes	6	2
Fgf3/Fgf4	7F5	7	9	Yes	38	—
Fgf8	19C3	5	4	Yes	15	—
Wnt3a	11B1.3	5	4	Yes	10	—
Irs4	XF2	3	4	Yes	—	—
Gm26870 (lincRNA)/Mir101c	9A1	1	6	No	—	—
Metln1/Ptchd3	11E2	3	3	Yes	—	—
Gm10800/Gm10801	2E1	1	5	No	—	—
Lrfn5	12C1	1	4	No	—	—
Astn2	4C1	2	2	Yes	2	—
Fgfr2	7F3	2	2	Yes	—	—
Map3k8	18A1	1	3	Yes	16	—
Wnt3	11E1	1	3	Yes	14	—
Gpc6/Gpc5	14E4	3	1	No	—	—
Zfp521	18A1	3	1	No	7	—
Sfi1	11A1	1	2	Yes	—	—
Fgfr1	8A2	2	1	Yes	—	—
Nova1	12B3	2	1	No	—	—
Ywhaq	12A1.3	2	1	No	—	—
Pdgfrb	18E1	0	2	Yes	—	—
Arf6	12C2	2	0	No	4	—
Arpm1 (Actrt3)	3A3	2	0	No	—	—
Btg1	10C3	2	0	No	—	—
Ctif	18E3	2	0	No	—	—
Dnah1	14B	2	0	No	—	—
Fhit	14A1	2	0	No	—	2
Id2	12A1.3	2	0	No	3	—
Mid1	XF5	2	0	No	7	—
Mme	3E1	2	0	No	—	—
Osbp15	7F5	2	0	No	—	—
Osbp18	10D1	2	0	No	—	—
Runx1	16C4	2	0	No	9	—
Slc25a25	2B	2	0	No	—	—

Chr. chromosome, — no CIS reported

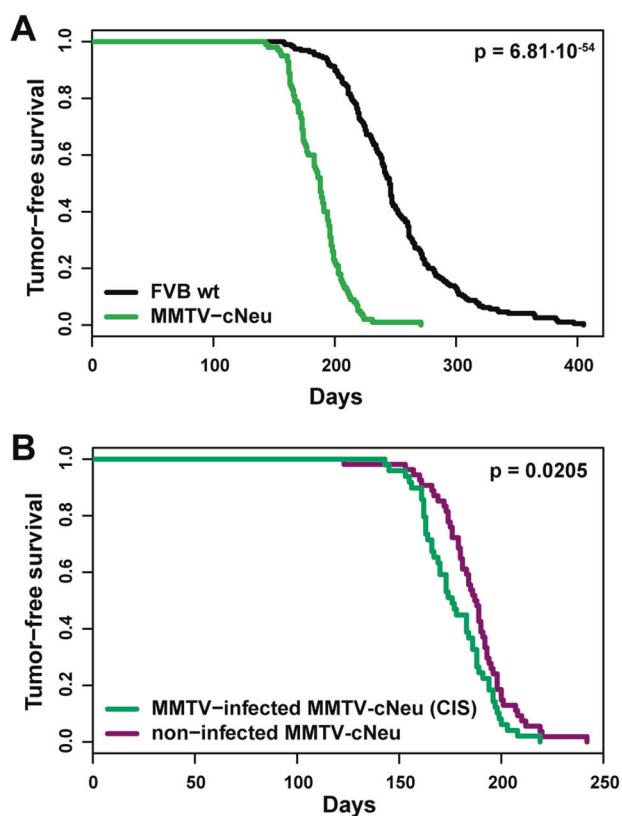


Fig. 1 Impact of MMTV infection on tumor free survival of *MMTV-cNeu* and wildtype FVB mice. **a**, **b** Kaplan–Meier curves of the MMTV-infected *MMTV-cNeu* mice ($n = 100$) compared to the MMTV-infected parental FVB wildtype strain ($n = 195$) (**a**) and MMTV-infected *MMTV-cNeu* mice with tumors carrying insertions in common insertion sites (CIS) ($n = 49$) compared to non-infected *MMTV-cNeu* mice ($n = 54$) (**b**). Statistical significance of differences in latency was determined by the pairwise log-rank test applying the *survdiff* function in R (p -values in upper-right corner). All mice eventually developed tumors and only mice that prematurely died from other causes were excluded

ERAS is a member of the RAS-family of small GTPases containing amino acid sequences identical to those present in constitutive active mutants of HRAS (e.g., HRasV12) and is therefore in a permanently active (GTP-bound) state [20, 21]. Mouse *Er*as is only expressed in embryonic stem (ES) cells and appears to be responsible for the tumor-like growth properties of ES cells when growing ectopically [21]. In addition, ERAS was reported to be required for somatic cell reprogramming to generate induced pluripotent stem (iPS) cells and the differentiation of ES cells into specific lineage cells [22–24]. In all these processes, the activation of the PI3K/AKT pathway by ERAS has been implicated, in contrast to the MAPK/ERK pathway generally activated by other RAS-family members.

Here, we report that *ERAS* is an oncogenic driver that acts synergistically with *ErbB2* in mammary tumorigenesis. Moreover, we show that *ERAS* expression occurs in a

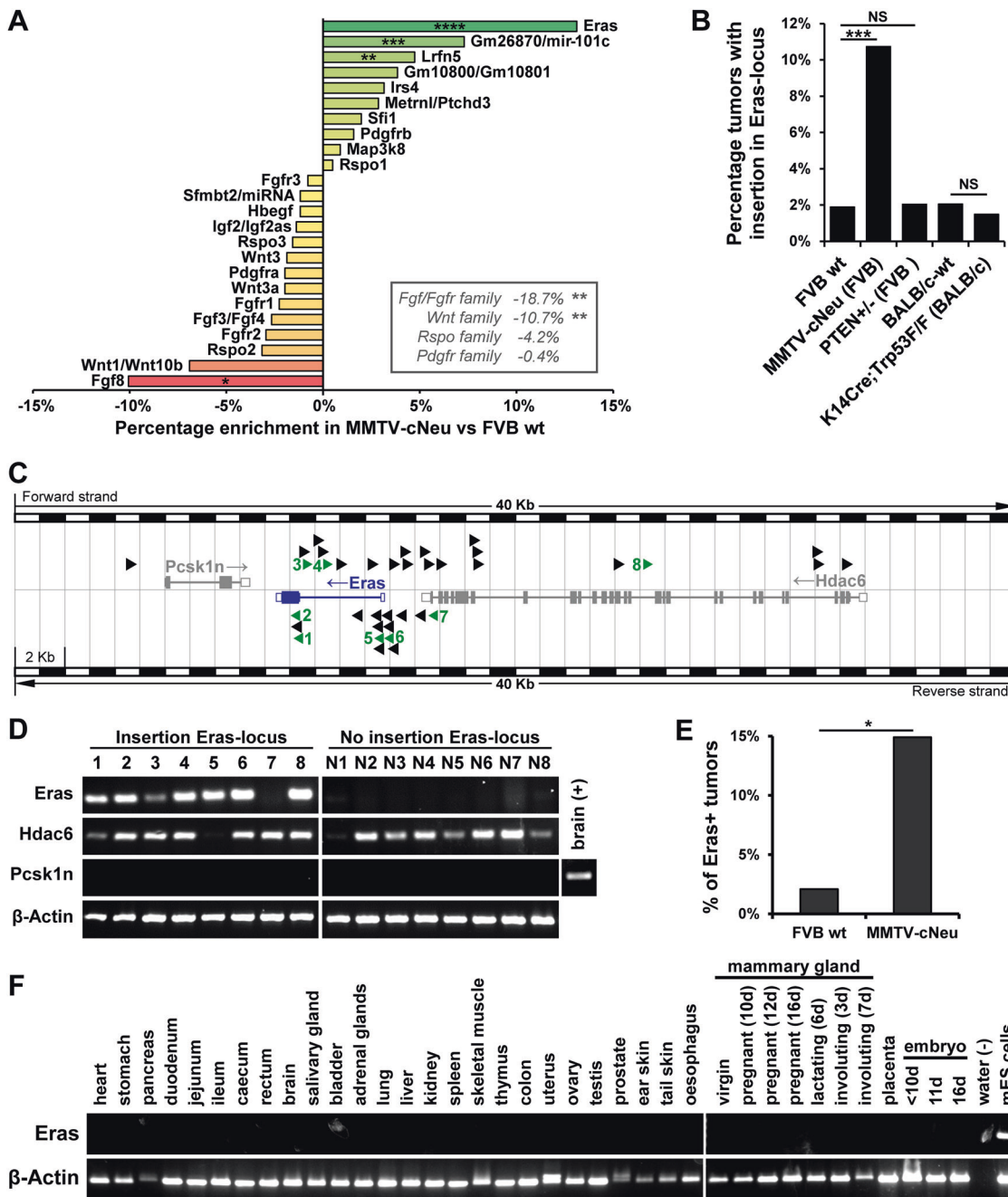
sizeable fraction of human HER2+ breast cancers. Finally, ERAS confers resistance to the HER2-targeted therapeutic agents Trastuzumab and Lapatinib through potent PI3K/AKT pathway activation.

Results

MMTV insertional mutagenesis in ErbB2+ predisposed background

We performed high-throughput sequencing of MMTV integration sites in mammary tumors obtained from MMTV-infected FVB mice, transgenic for rat *ErbB2* (*neu*) driven by the MMTV-promoter (*MMTV-cNeu* strain). We employed both the classical splinkerette PCR method and the more advanced “Shear-Splink” technology combined with the Gaussian Kernel Convolution framework in the Insertional Mutagenesis Database (iMDB; <http://imdb.nki.nl>) pipeline. To discriminate MMTV insertions that activate genes driving tumorigenesis from passenger insertions, we identified the CISs among independent tumors. In total, the screens yielded 34 CISs, of which 23 (68%) were found in both screens (Table 1). Twenty CISs have not been previously identified as an MMTV target, of which 14 have additionally not even been reported as CIS in the Retrovirus and Transposon tagged Cancer Gene Database (RTCGD; <http://variation.osu.edu/rctgd/>) [25] (Table 1).

We compared the results in the *MMTV-cNeu* transgenic mice obtained with the “Shear-Splink” setup in the present screen with the results from an identical screen in the parental FVB wildtype strain published earlier by our group [14]. Although the median tumor latency of the MMTV-infected *MMTV-cNeu* transgenic mice (188 days) was strongly decreased when compared to wildtype FVB mice infected with MMTV (245 days) (Fig. 1a), there was no significant difference in tumor latency between MMTV-infected and uninfected *MMTV-cNeu* mice. However, only 39% (59/151) of the independent tumors from MMTV-infected *MMTV-cNeu* mice contained an MMTV insertion belonging to a CIS in *MMTV-cNeu* mice, compared to 93% in MMTV-infected FVB wildtype mice [14]. This indicates that tumorigenesis driven by the predisposed background is in strong competition with tumorigenesis driven by MMTV insertional mutagenesis. When comparing only the MMTV-infected *MMTV-cNeu* mice with tumors driven by a CIS, the median latency was significantly decreased (176 days) compared to uninfected *MMTV-cNeu* mice (188 days) (Fig. 1b), suggesting that at least part of the CIS-associated MMTV integrations may accelerate mammary tumorigenesis in *MMTV-cNeu* mice in collaboration with the *ErbB2*-transgene.



MMTV target Eras is associated with the ErbB2/Neu genotype

Loci harboring genes of the *Wnt*, *Fgf*, and *Fgfr*-family were among the most frequent CISs (Table 1), but these loci are also frequent hits in wildtype FVB, BALB/c, and other mouse strains [11, 13, 14], and thus unlikely to be specific to the *ErbB2*-transgenic (*MMTV-cNeu*) genotype. Comparing the CIS-frequency in the *ErbB2*-transgenic FVB mouse models with the CIS-frequency in its parental FVB wildtype strain, revealed even a significantly negative correlation of

the *Wnt* and *Fgf/Fgfr*-family CISs with the *MMTV-cNeu* genotype ($p = 7.64 \times 10^{-3}$ and $p = 1.48 \times 10^{-3}$, respectively, Fisher's exact test) (Fig. 2a). Three CISs, however, significantly associated with the *ErbB2*-genotype, including the loci containing *Lrfn5* (leucine-rich repeat and fibronectin type III domain-containing 5), the long intergenic non-coding RNA *Gm26870* or microRNA-101c (*Mir101c*), and especially *Eras* (ES cell-expressed Ras) ($p = 3.57 \times 10^{-3}$, $p = 1.06 \times 10^{-4}$ and $p = 3.08 \times 10^{-7}$, respectively, Fisher's exact test). More CISs may be associated with *ErbB2*-overexpression, considering that, e.g., the *Irs4*-locus

Fig. 2 *Eras* is an MMTV target associated with the *ErbB2/Neu* genotype. **a** Enrichment of MMTV CISs in *cNeu*-transgenic FVB mice compared to FVB wildtype mice, calculated as percentage of all independent tumors in each group. The same analysis for gene families are shown in the lower-right corner. Significance of positive or negative enrichment was determined by a Fisher's exact test and *p*-values are shown as **p* < 0.05; ***p* < 0.01; ****p* < 0.001; *****p* < 1×10^{-4} . See also Supplementary Table 2. **b** Percentage of independent tumors with an MMTV insertion in the *Eras* locus for the mouse strains: FVB wildtype (*n* = 265), *MMTV-cNeu* (*n* = 177), *PTEN* +/− (*n* = 196), BALB/c wildtype (*n* = 292), and *K14Cre;Trp53^{FF}* (*n* = 202). Statistical significance of differences in relevant comparisons was determined by a Fisher's exact test: NS not significant; ****p* < 0.001. **c** Map of MMTV integrations in the *Pcsk1n/Eras/Hdac6*-locus on the X-chromosome, showing the gene names (arrow heads indicate orientation), their translated exons (solid rectangles), UTRs (open rectangles), and the interspersing introns (lines). MMTV-proviral insertions are indicated with triangles pointing in the orientation of integration. Green arrow heads represent tumors analyzed in **d**. **d** RT-PCR expression analysis of *Eras*, *Pcsk1n*, and *Hdac6* in tumors with integration in the *Pcsk1n/Eras/Hdac6*-locus, following the numbering of **c** and random tumors without integrations in this locus (the rest of the analysis is provided in Supplementary Fig. 1A). PCR-products for β -actin were used as controls for RNA integrity. **e** Percentage of *Eras*-mRNA expressing independent MMTV-induced tumors from FVB wildtype mice (*n* = 48) and *cNeu*-transgenic FVB mice (*n* = 161), showing that *Eras* is significantly more commonly expressed in tumors from *cNeu*-transgenic mice; *p*-value = 0.01973 (*), determined by a Fisher's exact test. **f** *Eras*-mRNA expression in tissues from BALB/c wildtype mice, including tissues from various stages of mammary gland development and embryogenesis (showing days), determined by RT-PCR. A sample of murine ES cells was used as positive control and β -actin expression was assessed as control for RNA integrity

here only shows a trend towards enrichment in the *ErbB2* genotype (Fig. 2a), whereas we recently reported that *IRS4* collaborates with *ERBB2* in tumorigenesis [15, 26]. When relating the MMTV integration data reported here with those of our previously published screens [11, 14], integrations in the *Eras* locus were far more common in the *MMTV-cNeu* genotype compared to the FVB wildtype strain ($p = 1.28 \times 10^{-4}$, Fisher's exact test), and also compared to the BALB/c wildtype, *K14Cre;Trp53^{FF}* (BALB/c background), and *PTEN*^{+/-} mice (FVB background) (Fig. 2b). This indicates that integrations in the *Eras* locus provides a selective growth advantage especially in *ErbB2* transgenic mice.

On the basis of the genomic location and orientation of the MMTV-proviral integrations in the *Eras* locus, *Eras* is the most likely gene candidate to be transcriptionally activated (Fig. 2c), but the locus also contains the *Pcsk1n* (proprotein convertase subtilisin/kexin type 1 inhibitor) and *Hdac6* (histone deacetylase 6) genes that could also be transcriptionally activated by the MMTV insertions. To determine the actual MMTV target gene(s), we performed a side-by-side analysis of *Pcsk1n*, *Eras*, and *Hdac6* mRNA expression in eight *MMTV-cNeu* tumors with and 32 tumors without MMTV-proviral insertion in the *Eras* locus using

RT-PCR (Fig. 2d; Supplementary Fig. 1A). *Pcsk1n* was not expressed in any of the tumors, excluding this gene as the MMTV target. *Hdac6* mRNA was present in all but one of the tumors from both groups, regardless of the presence of an MMTV insertion in the *Eras* locus. Moreover, also MMTV-induced mammary tumors from FVB wildtype mice and spontaneous tumors from *ErbB2* transgenic mice were almost all positive for *Hdac6* mRNA (Supplementary Fig. 1B, C), indicating that expression of *Hdac6* is rather ubiquitous in mouse mammary tumors and not correlated to MMTV integrations in the *Eras* locus. Only *Eras* expression was clearly correlated with MMTV integration in the locus ($p = 1.023 \times 10^{-4}$, Fisher's exact test), showing expression in all but one tumor with an MMTV integration in the *Eras* locus, whereas no clear expression was observed in tumors without integration.

As our stringent method of assigning integration sites—designed to limit false-positive findings—inherently produces false-negatives in our screens, the number of integrations we report is likely an underestimation. Therefore, we compared *Eras*-gene expression in a panel of 161 tumors from MMTV-infected *ErbB2* transgenic FVB mice (including those in Fig. 2d and Supplementary Fig. 1A) with the expression in a panel of 48 tumors from MMTV-infected wildtype FVB mice. In accordance with our previous results, we found that *Eras* was significantly more frequently expressed in MMTV-induced tumors from *ErbB2*-transgenic mice (15%) compared to wildtype mice (2%) (Fig. 2e). This strongly suggests that *Eras* specifically collaborates with *ErbB2* in mammary tumorigenesis.

Importantly, we observed no *Eras* expression during any stage of murine mammary gland development, nor in any other mouse tissue or during embryogenesis (from ~E9 onwards). In line with previous reports [21], we exclusively observed expression of the gene in ES cells, indicating that *Eras* is strictly regulated at the transcriptional level (Fig. 2f).

ERAS stimulates cell proliferation synergistically with ERBB2

To investigate the biological basis of the revealed oncogenic collaboration between *Eras* and *ErbB2*, we ectopically expressed *ERAS* in the human HER2+ (amplified wildtype *ErbB2*) breast cancer cell line SKBR3. We observed a strongly increased cell proliferation rate in cells transduced with *ERAS* compared to vector controls (Fig. 3a; Supplementary Fig. 2A). To assess the contribution of *Eras* and *ErbB2*, separately and in combination, we compared the proliferation rates of the spontaneously immortalized normal mammary epithelial cell line NMuMG transduced with *Eras* and *ErbB2* individually, *Eras* and *ErbB2* combined, or the empty vector control under various growth conditions

Fig. 3 ERAS promotes cell proliferation synergistically with ERBB2. **a** Growth curves based on Crystal Violet staining of SKBR3 cells ectopically expressing *ERAS* compared to vector control cells, showing mean \pm SD cell density, relative to day 0 ($n = 3$) (25,000 cells per well, 12-wells plates). Micrographs of these cells at day 9 are provided in Supplementary Fig. 2A. **b** Western blot showing human and murine ERAS protein in NMuMG cells stably transduced with human or murine *ERAS* (hERAS or mEras, respectively), *ErbB2* alone, *ErbB2* and *ERAS*, or the empty vector. β -actin was used as loading control. This anti-ERAS antibody did not react with HRas or KRas (see Supplementary Fig. 2B). These results were confirmed with another antibody for ERAS (see Supplementary Fig. 2C). **c** Growth curves of NMuMG cells as in **b** under normal growth conditions (10% FBS + insulin), without insulin or under low serum conditions (0.5% FBS), based on Crystal Violet staining (30,000 cells per well, 12-wells plate). Plotted values are mean \pm SD, relative to day 0 ($n = 3$)

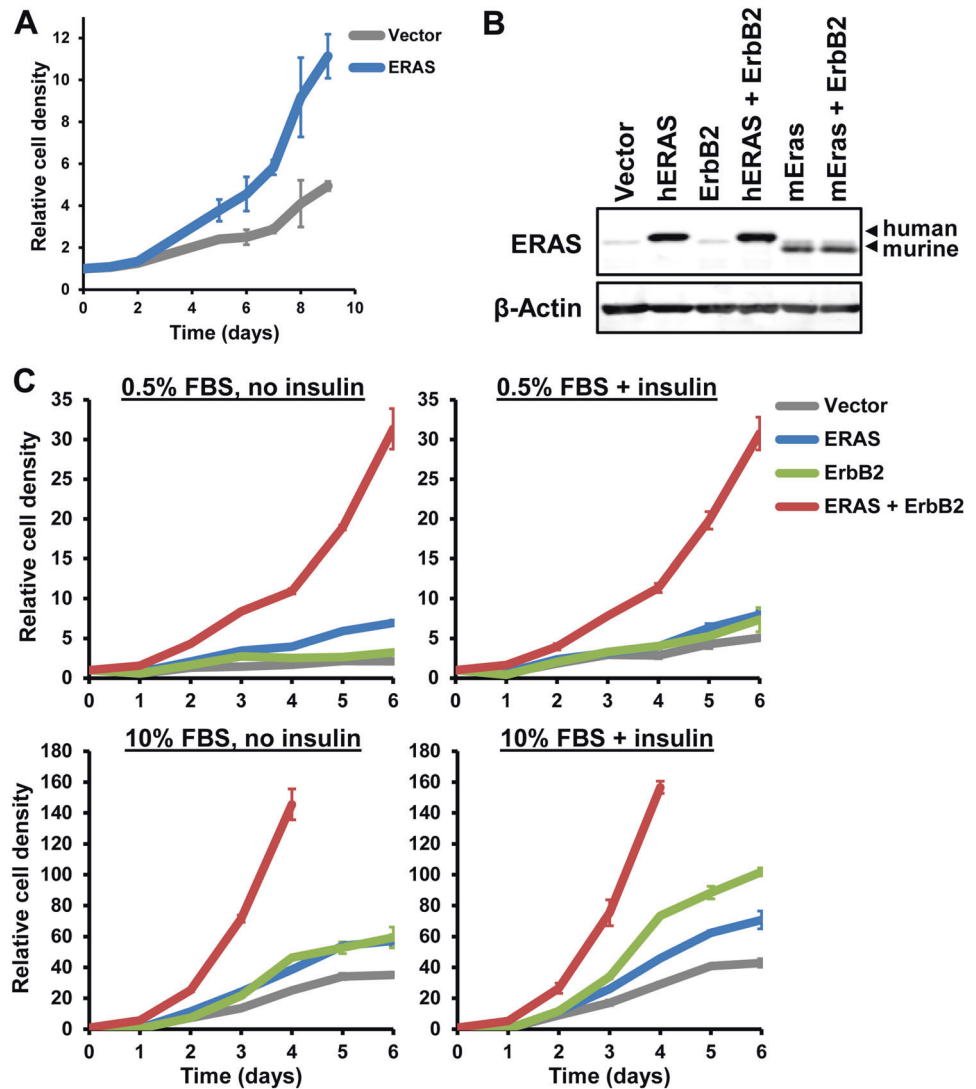
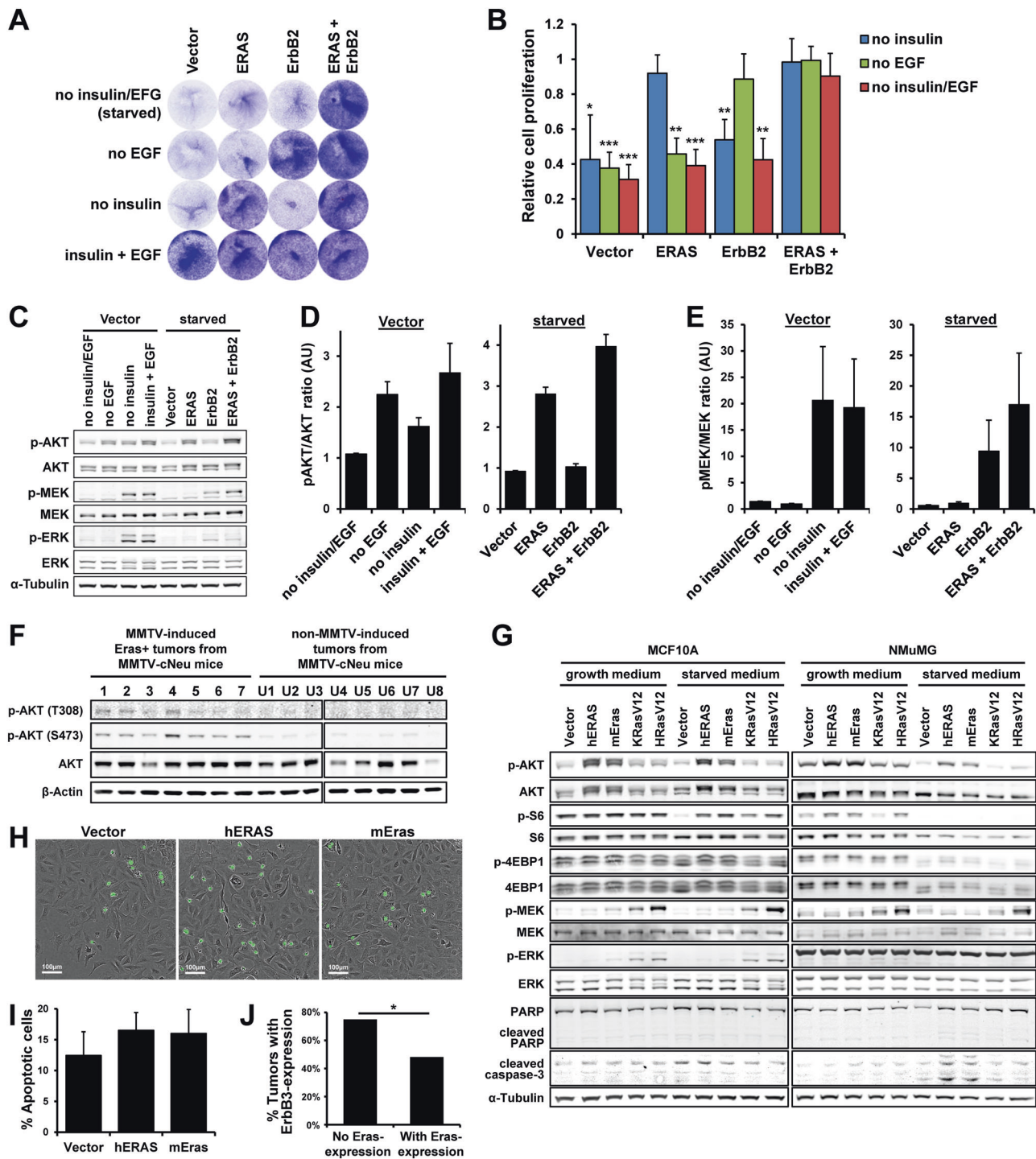


(Fig. 3b, c; Supplementary Fig. 2B, C). Under all growth conditions, *Eras*-expressing NMuMG cells showed a higher cell proliferation rate than the vector control. Moreover, cells expressing *Eras* appeared to be independent of insulin for growth, in contrast to cells that lacked *Eras* expression. NMuMG cells transduced with *ErbB2* alone showed an increased cell proliferation rate, but not under low serum conditions (0.5%). However, when both *Eras* and *ErbB2* were expressed in these cells, cell proliferation was synergistically increased under all tested conditions. Similar results, including the drastic enhancement of cell proliferation by combined expression of *ERAS* and *ErbB2*, were obtained with the human breast epithelial cell line MCF10A, using either murine or human *ERAS* (Supplementary Fig. 2D). Thus, co-expression of *ERAS* and *ErbB2* synergistically enhances cell proliferation of mammary epithelial cells.

ERAS and ERBB2 collaborate by activating complementary pathways

To further investigate the observed insulin-independence of cells expressing *ERAS* and the mechanism of synergism with *ErbB2*, we grew MCF10A cells with and without these genes in near absence of serum (0.1%) and we omitted insulin and EGF from the medium, growth factors that are normally required for growth of these cells (a third factor, hydrocortisone, was always added). Empty vector control cells were unable to grow in absence of either insulin or EGF (Fig. 4a, b), whereas expression of *ERAS* or *ErbB2* provided the cells with the capability to grow in the absence of insulin or EGF, respectively. Co-expression of *ERAS* and *ErbB2* enabled cellular growth in medium depleted from serum, EGF and insulin. EGF primarily functions through the MAPK/ERK pathway via EGFR, whereas insulin



predominantly activates the PI3K/AKT signaling cascade through the insulin receptor (Fig. 4c–e). We therefore hypothesized that ERAS and ERBB2 collaborate through the activation of these complementary pathways. Indeed, it has been shown that *ERAS* expression activates the PI3K/AKT pathway in mouse ES cells [21]. Here, we show that also in mammary epithelial cells, expression of *ERAS* strongly induces PI3K/AKT-pathway activity, as

determined by AKT phosphorylation (Fig. 4c, d). Moreover, MMTV-induced *Eras* expression in primary mammary tumors additionally correlates with PI3K/AKT-pathway activation (Fig. 4f). Although *ErbB2* expression alone appears to exclusively activate the MAPK/ERK pathway, its co-expression with *ERAS* additionally enhances PI3K/AKT pathway activity (Fig. 4c, e; Supplementary Fig. 3A).

Fig. 4 ERAS and ERBB2 activate complementary signaling pathways. **a** Representative Crystal Violet staining of MCF10A cells, stably transduced with *ERAS* and *ErbB2* alone or co-expressed, compared to vector control cells. 200,000 cells per well (6-wells plates) were allowed to grow for 4 days in medium supplemented with 0.1% FCS, with and without insulin and EGF (as indicated). **b** Quantification of cell proliferation in **a**, relative to the growth condition with both insulin and EGF ($n = 4$), plotted as mean + SD. Significant differences in cell proliferation rates upon omission of growth factors are shown and were determined by a Welch's *t*-test and *p*-values are shown as * $p < 0.05$; ** $p < 0.01$; *** $p < 0.001$. **c** Representative Western blots showing phosphorylated (p-) and total protein of AKT, MEK, and ERK in MCF10A vector control cells in medium with and without insulin and EGF (as indicated), compared to MCF10A cells in medium devoid of those growth factors (starved), stably transduced with *ERAS* and *ErbB2* alone or in combination (as indicated). All proteins were detected on the same blot and α -tubulin was used as loading control. **d**, **e** Ratios phosphorylated over total AKT (**d**) and MEK (**e**), plotted as mean + SD ($n = 3$) and quantified from the blots as in **c**. pERK/ERK ratios are provided in Supplementary Fig. 3A. **f** Western blots showing phosphorylated (p-)AKT (on the indicated amino acid residues) and total AKT protein in tumors with MMTV induced *Eras* expression and in non-MMTV induced tumors that arose in *ErbB2* transgenic mice. β -actin was used as loading control. **g** Western blots showing PI3K/AKT (AKT, S6, 4EBP1), MAPK/ERK (MEK, ERK), and apoptosis (PARP, caspase-3) signaling in MCF10A and NMuMG cells, stably transduced with human or murine *ERAS* (hERAS or mEras, respectively), *KRASV12* or *HRASV12*, compared to vector control cells. Cells were grown under starved conditions or in complete growth medium. All proteins were detected on the same blot and α -tubulin was used as loading control. **h** Representative micrographs showing apoptosis in green (fluorescent caspase-3/7 reagent) of 7-day starved MCF10A cells, stably transduced with human or murine *ERAS* (hERAS or mEras, respectively) and vector control cells (scale bar = 100 μ m) (1500 cells per well, 384-wells plates). The same analysis in NMuMG cell is provided in Supplementary Fig. 3B. **i** Quantification of percentages apoptotic cells of experiment in **h**, showing mean + SD ($n = 4-7$). Welch's *t*-test showed no significant differences ($p > 0.05$). The same analysis in NMuMG cell is provided in Supplementary Fig. 3C. **j** Percentage of *ErbB3*-expression positive MMTV-induced tumors in tumors with ($n = 52$) or without ($n = 27$) *Eras* expression, showing a statistically significant difference with p -value = 0.0244 (*), determined by a Fisher's exact test

We explored possible differences in signaling downstream of ERAS compared to other oncogenic RAS-family members. Although ERAS induced potent activation of the PI3K/AKT pathway in mouse mammary cells, it did not activate the MAPK/ERK pathway, in contrast to constitutive active mutants of canonical oncogenic RAS-family members KRAS (KRASV12; Kirsten rat sarcoma viral oncogene homolog) and HRAS (HRASV12; Harvey rat sarcoma viral oncogene homolog) that primarily activated the MAPK/AKT pathway (Fig. 4g: p-AKT, p-ERK, and p-MEK).

ERAS could potentially also protect against apoptosis and hence in part explain the observed ERAS-induced cell expansion. However, cells expressing *ERAS* showed slightly more activation of the apoptosis signaling cascade, which was confirmed microscopically (Fig. 4g-i;

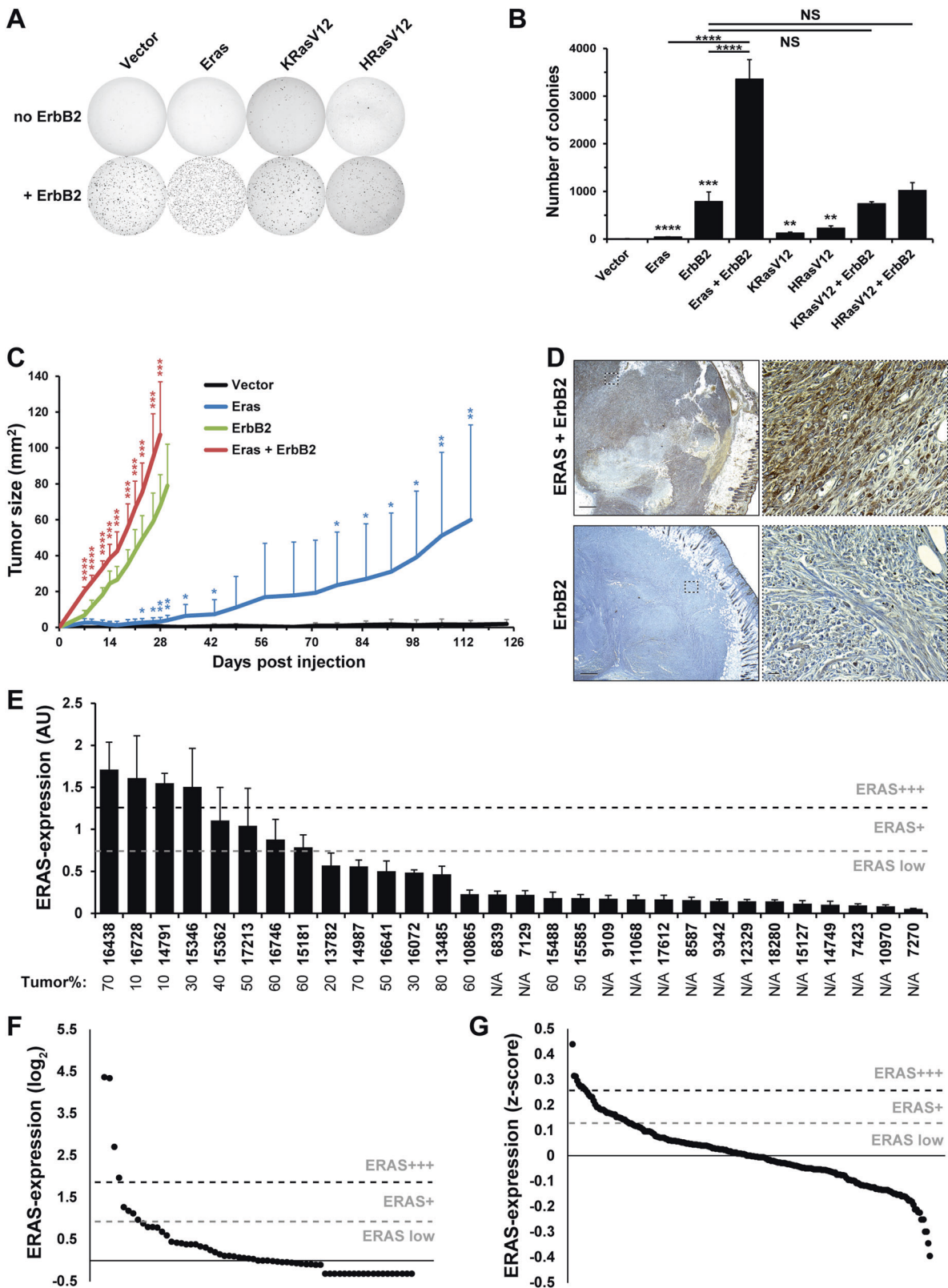
Supplementary Fig. 3B, C). Thus, ERAS does not protect cells from apoptosis, but does strongly induce cell proliferation via PI3K/AKT pathway activation.

ERBB2 forms homo- or heterodimers with other ERBB-family members, most notably with ERBB3 (erb-b2 receptor tyrosine kinase 3). In this complex, ERBB3 is required for PI3K/AKT pathway signaling and thereby strongly contributes to tumorigenesis [27, 28]. As we established that ERAS is a very potent activator of the PI3K/AKT pathway, we hypothesized that it may functionally replace ERBB3. Indeed, we find significantly less *ErbB3*-expression among the *Eras*-positive tumors arising in MMTV-infected *ErbB2*-transgenic mice, compared to *Eras*-negative tumors (Fig. 4j). Other MMTV target genes may also be able to replace *ErbB3*, as we find that 42% of MMTV-induced *ErbB2*-driven tumors lack *ErbB3*-expression, whereas all spontaneous *ErbB2*-driven tumors expressed *ErbB3* (Supplementary Fig. 3D).

ERAS collaborates synergistically with ERBB2 in tumorigenesis

To assess whether the collaboration of ERAS with ERBB2 indeed affects tumorigenic potential, we performed a soft agar colony formation assay, as anchorage-independent growth correlates well with in vivo tumorigenicity (Fig. 5a, b; Supplementary Fig. 4A, B). Both in MCF10A and NMuMG cells, expression of *ERAS* hardly enabled anchorage-independent growth, whereas *ErbB2*-expression did induce some colony formation. Combined expression of *ERAS* and *ErbB2*, however, resulted in a strong synergistic induction of anchorage-independent growth in these cells. Interestingly, this synergism was not observed between ERBB2 and constitutive active KRAS (KRASV12) or HRAS (HRASV12) (Fig. 5b). Hence, the synergistic tumorigenic collaboration with ERBB2 seems unique to ERAS within the RAS family. Moreover, ERAS seems able to functionally replace ERBB3 in induction of anchorage-independent growth in collaboration with ERBB2 (Supplementary Fig. 4C).

To further validate the observed oncogenic synergism between ERAS and ERBB2, we investigated whether combined expression of *ERAS* and *ErbB2* in NMuMG cells indeed synergistically enhances tumor growth in vivo. To this end, we subcutaneously injected 1×10^6 NMuMG cells transduced with *ERAS* and *ErbB2*, alone or in combination, or vector control cells in both flanks of five female BALB/c nude mice and compared tumor latency and growth (Fig. 5c). All mice injected with *Eras*-transduced cells developed tumors in both flanks, whereas mice injected with the vector control cells did not develop any tumors, even after a prolonged time period, implying that expression of *Eras* alone is already oncogenic in mammary



epithelial cells. *ErbB2*-expressing cells were tumorigenic as expected, but combined with *Eras* expression, with confirmed ERAS protein expression (Fig. 5d), strongly

accelerated tumor growth (Fig. 5c), providing in vivo evidence that ERAS and ERBB2 indeed synergistically collaborate in tumorigenesis.

Fig. 5 ERAS and ERBB2 synergistically induce tumor growth. **a** Representative whole well scans of NMuMG cells, stably transduced with *Eras*, *KRasV12*, or *HRasV12* alone or co-expressed with *ErbB2*, allowed to grow in soft agar for three weeks (25,000 cells per well, 6-wells plates). **b** Quantification of soft agar growth of **a**, plotted as mean + SD ($n = 4-6$). Statistical significance of differences in relevant comparisons was determined by a Welch's *t*-test and *p*-values are shown as * $p < 0.05$; ** $p < 0.01$; *** $p < 0.001$; **** $p < 1 \times 10^{-4}$; NS not significant. Relevant significant differences to the vector control are depicted above the columns. **c** Tumor growth in mice subcutaneously injected with NMuMG cells ectopically expressing *ERAS* and *ErbB2* alone or in combination, and vector control cells ($n = 10$ each). Data are represented as mean + SD. Statistically significant differences in tumor growth between vector controls and *Eras* (blue) or *ErbB2* and *Eras* + *ErbB2* (red) are indicated as * $p < 0.05$; ** $p < 0.01$; *** $p < 0.001$; **** $p < 1 \times 10^{-4}$ (Welch's *t*-test). **d** Representative micrographs of immunohistochemical staining for *ERAS* (brown) in tumors grown from subcutaneously injected NMuMG cells, stably transduced with *ErbB2* with or without *Eras*, described in **c**. Right panels are enlargements of the boxed areas. Scale bars: overviews (left) = 500 μm , details (right) = 20 μm . **e** Quantitative RT-PCR of *ERAS* mRNA expression in 30 HER2-positive primary breast carcinomas. Lower thresholds for *ERAS* positive (*ERAS*+; above median + SD) and highly positive (*ERAS*+++; above median + 2 \times SD) are indicated with a gray and black dashed line, respectively. The estimated tumor percentages are indicated below each sample: N/A, not available. **f, g** Median-centered *ERAS* mRNA expression levels in HER2-positive tumor samples (based on PAM50 gene signature) derived from The Cancer Genome Atlas (TCGA) RNA-seq data ($n = 65$) [29] (**f**) or METABRIC microarray data ($n = 220$) [30] (**g**). Thresholds for *ERAS* positive (*ERAS*+) and highly positive (*ERAS*+++ expression levels are indicated as in **e**

ERAS is expressed in a subset of human primary breast carcinomas

To determine the clinical significance of *ERAS*, we used RT-PCR to examine the expression of *ERAS* mRNA in a large group of primary human breast carcinomas from patients treated in our institute (Supplementary Fig. 4D; Supplementary Table 1). Five out of 51 tumors (10%) showed clear *ERAS* expression, confirmed by immunohistochemistry (Supplementary Fig. 4E), and an additional nine breast cancer samples exhibited lower levels of *ERAS* mRNA. Sequencing of the PCR-products excised from the gel confirmed that the amplified cDNA represented *ERAS* mRNA of human origin. Surprisingly, only few of the *ERAS*-positive tumors were also categorized as HER2+ (Supplementary Table 1), where we would expect an enrichment of *ERAS* positive tumors, based on our in vitro and in vivo studies. We therefore tested an independent uniform HER2+ human breast cancer series for *ERAS* expression by quantitative RT-PCR (Fig. 5e). Eight out of the 30 tested HER2+ tumors (27%) could be scored as *ERAS* positive, of which four cases (13%) were highly positive. This may even be an underestimation due to the low tumor percentage in some of the samples (Fig. 5e). We did not observe samples with both high expression of *ERAS*

and *ERBB3* (Supplementary Fig. 4F, G), strengthening our notion that *ERAS* may functionally replace *ERBB3*. The publicly available expression datasets of The Cancer Genome Atlas (TCGA) (RNA-seq) [29] and METABRIC (microarray) [30] both confirm *ERAS* expression in a subset of human HER2+ breast cancers, albeit with somewhat lower percentages (TCGA: 12% *ERAS*+, 6% *ERAS*+++; METABRIC: 16% *ERAS*+, 7% *ERAS*+++ (Fig. 5f, g). These results point at a role for this intrinsically active and oncogenic RAS-like gene in human breast cancer.

ERAS induces resistance to HER2-targeting therapy

Although HER2-targeting therapy has improved clinical outcome, therapy resistance remains a considerable problem in the clinic. Previously, PI3K/AKT pathway hyperactivation has been associated with therapy resistance in HER2+ breast cancer [31–33]. As our data show that *ERAS* constitutively activates this pathway, we interrogated whether expression of *ERAS* could also alter the response to HER2-targeting therapy. Indeed, we found that *ERAS* expression in the HER2+ breast cancer cell lines SKBR3 and BT474, leads to a marked reduction in sensitivity to both the *ERBB2*-targeting monoclonal antibody Trastuzumab and the small molecule *ERBB2*-kinase inhibitor Lapatinib, enabling sustained tumor cell growth (Fig. 6a–c; Supplementary Fig. 5A, B).

To confirm that the mechanism of therapy resistance by *ERAS* is due to its potent PI3K/AKT pathway activation, we treated HER2+ breast cancer cell lines with suboptimal concentrations of Trastuzumab or Lapatinib, in combination with the PI3K inhibitor GDC-0941 (Fig. 6d, e; Supplementary Fig. 5C–E). Although single-agent treatments had little to no influence on the proliferation rate of breast cancer cells expression both *ERBB2* and *ERAS*, the combination of HER2- and PI3K-targeting agents potently reduced cell proliferation. These data strongly suggest that PI3K/AKT-pathway activation by *ERAS* confers resistance to HER2-targeting therapeutics. Moreover, these data further support our conclusion that the observed synergism between *ERBB2* and *ERAS* in tumorigenesis is due to their activation of the complementing oncogenic MAPK/ERK and PI3K/AKT pathways, respectively.

To validate *ERAS*-induced resistance in vivo, we subcutaneously injected 1×10^6 NMuMG cells expressing *ErbB2*, alone or in combination with *Eras*, in opposite flanks of 18 female BALB/c nude mice. When tumors had been established in both flanks, we randomly assigned nine mice to receive Lapatinib treatment (Fig. 6f, g). Tumor growth was significantly reduced upon Lapatinib treatment in flanks injected with cells only expressing *ErbB2*. In contrast, tumors expressing both *ErbB2* and *Eras* showed

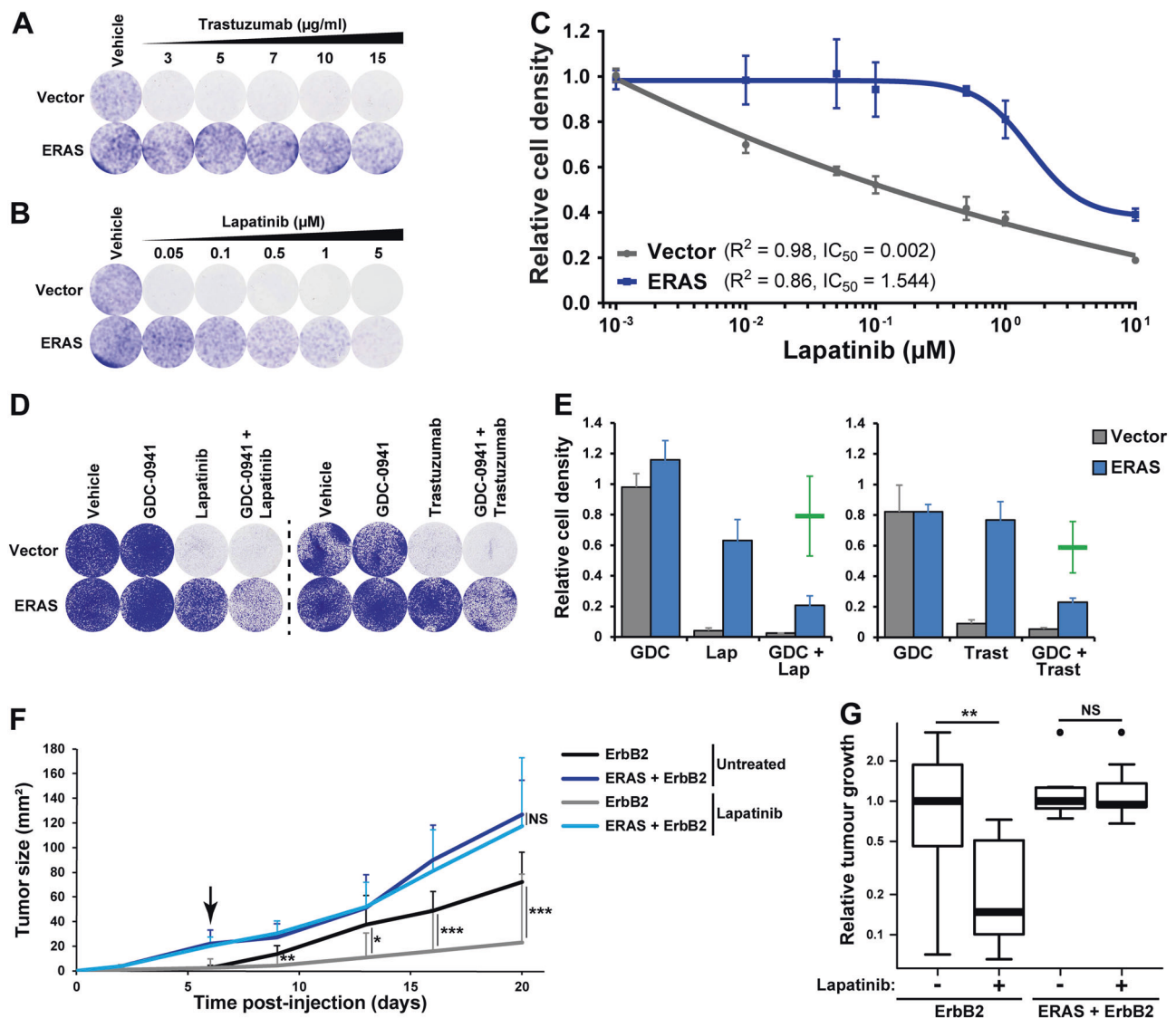


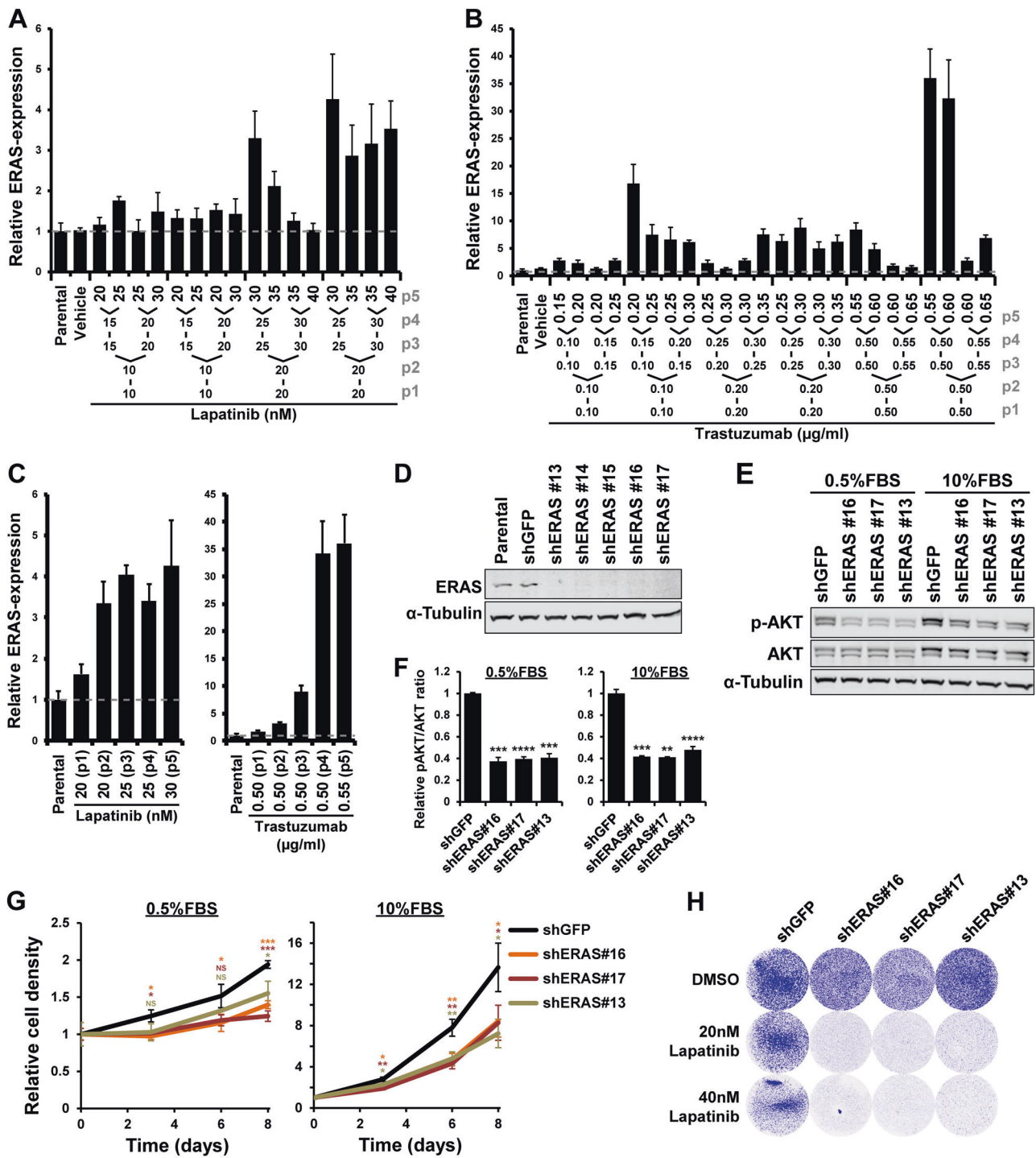
Fig. 6 ERAS induces Trastuzumab and Lapatinib resistance via PI3K/AKT-pathway hyperactivation. **a, b** Crystal Violet staining of BT474 vector controls or BT474 cells stably transduced with *ERAS*, allowed to grow for 7 or 10 days in medium supplemented with the indicated concentrations Trastuzumab (**a**) or Lapatinib (**b**), respectively (25,000 cells per well, 24-wells plates). **c** Lapatinib dose response curves of SKBR3, stably transduced with *ERAS*, or vector control cells. The data points represent the mean \pm SD ($n=4$) of the cell density of the Lapatinib-treated to vehicle control cells (initially, 1000 cells per well were plated, 384-wells plate). The fitted curve and associated R^2 and IC_{50} values are shown. **d** Representative Crystal Violet staining of BT474 vector controls or BT474 cells stably transduced with *ERAS*, grown in presence of 20 nM Lapatinib (grown 13 days), 5 μ g/ml Trastuzumab (grown 11 days) and/or 20 nM PI3K inhibitor GDC-0941, or equal volumes of DMSO (vehicle) (50,000 cells per well, 12-

wells plates). **(e)** Quantification of **(d)**, showing cell proliferation relative to vehicle controls. Data plotted as mean \pm SD ($n=3$). A projection of the combined (i.e., additive) single-agent effects of GDC-0941 (GDC) and Lapatinib (Lap) or Trastuzumab (Trast) is shown in green. **f** Tumor growth of NMuMG cells, stably transduced with *ErbB2* alone or together with *ERAS*, subcutaneously injected in opposite flanks of BALB/c nude mice, untreated or treated with 100 mg/kg/day Lapatinib ($n=9$ each). When tumors were established in both flanks, mice were randomly allocated to either group before treatment was started (indicated by arrow). Significant differences in growth rate between treated and untreated tumors are determined by a Welch's *t*-test: * $p < 0.05$; ** $p < 0.01$; *** $p < 0.001$; NS not significant. **g** Boxplot of tumor growth from start of treatment to day 20 of experiment in **f**, relative to growth of untreated controls. Statistical analysis was performed by a Welch's *t*-test: ** $p < 0.01$; NS not significant

no response to Lapatinib, confirming ERAS-induced Lapatinib resistance in vivo.

In analogy to acquired therapy resistance in patients with HER2+ breast cancer, we investigated whether expression

of endogenous *ERAS* could also be attained in treatment-naive HER2+ breast cancer cell lines under selective pressure of Trastuzumab or Lapatinib. To this end, we cultured SKBR3 and BT474 cells in medium containing



increasing concentrations of Trastuzumab or Lapatinib. In more than half of the cultures, *ERAS* expression was induced within five passages in the presence of Trastuzumab or Lapatinib, especially at higher drug concentrations (Fig. 7a, b; Supplementary Fig. 6A, B). Detailed expression analysis of each passage revealed that *ERAS* expression increases gradually with every passage, indicating a selection for increasing *ERAS* expression by the increasing drug

concentrations (Fig. 7c; Supplementary Fig. 6C). In contrast, untreated control cells did not show increased *ERAS* expression after five passages. Subsequent knockdown of Trastuzumab-induced endogenous *ERAS* expression in BT474 and SKBR3 cultures with the highest induction (designated: BT474/R^{ERAS+} and SKBR3/R^{ERAS+}, respectively) resulted in a concomitant significant reduction in PI3K/AKT-pathway activation, cell proliferation and

Fig. 7 HER2-targeted treatment selects for cells expressing *ERAS*. **a, b** *ERAS*-mRNA expression levels in BT474 cells (parental), cultured for five passages in presence of vehicle (to aid interpretation of the graph this level is also indicated by a gray dashed line) or the indicated concentrations Lapatinib (**a**) or Trastuzumab (**b**). Data are represented as mean + SD of triplicates and are shown relative to *ERAS* levels in vehicle controls. Lapatinib or Trastuzumab concentrations after each passage are shown below and passage number (p) is depicted in gray at the right. The same experiment using SKBR3 cells is provided in Supplementary Fig. 6A and B. **c** Relative *ERAS*-expression levels at each passage in the cultures that acquired the highest *ERAS* levels under Lapatinib or Trastuzumab selection depicted in **a** and **b**, respectively. **d** Western blot, showing *ERAS* knockdown efficiency in the Trastuzumab-treated BT474 cell culture of **c** (designated: BT474/R^{ERAS+}). α -Tubulin was used as loading control. The same analysis in SKBR3 cells is provided in Supplementary Fig. 6C. **e** Representative Western blots showing phosphorylated (p-) and total protein of AKT in a selection of the cell cultures from **d**. α -Tubulin was used as loading control. **f** Ratios phosphorylated over total AKT, relative to shGFP controls, quantified from the blots as in **e**. Data represented as mean + SD ($n = 3$) and statistically significant differences in PI3K/AKT-pathway activation between shGFP controls and sh*ERAS* are indicated as ** $p < 0.01$; *** $p < 0.001$; **** $p < 1 \times 10^{-4}$ (Welch's *t*-test). The same experiment using SKBR3 cells is provided in Supplementary Fig. 6G. **g** Growth curves of the BT474/R^{ERAS+} cell culture as in **f** in medium supplemented with 10% FBS or 0.5% FBS, based on Crystal Violet staining (50,000 cells per well, 24-wells plates). Plotted values are mean \pm SD, relative to day 0 ($n = 3$). Statistical significance of differences in cell proliferation between shGFP controls and sh*ERAS* was determined by a Welch's *t*-test and *p*-values are shown as * $p < 0.05$; ** $p < 0.01$; *** $p < 0.001$; NS not significant. The same experiment using SKBR3 cells is provided in Supplementary Fig. 6H. **h** Representative Crystal Violet staining ($n = 3$) of the BT474/R^{ERAS+} cells as in **f**, allowed to grow for 6 days in the presence of 20 nM or 40 nM Lapatinib or equal volumes of vehicle (DMSO) (50,000 cells per well, 24-wells plates). The same experiment using SKBR3 cells is provided in Supplementary Fig. 6I

Lapatinib resistance (Fig. 7d–h; Supplementary Fig. 6D–I). These data further prove that induction of *ERAS* expression renders tumor cells insensitive to HER2-targeted therapy and as such present a new mechanism of therapy resistance.

Discussion

To shed more light on HER2+ breast tumorigenesis and the mechanisms underlying resistance to HER2-targeting therapeutics, we performed high-throughput MMTV-mediated insertional mutagenesis screens in an *MMTV-cNeu* transgenic mouse model for HER2+ human breast cancer to discover genes collaborating with ERBB2. Here, we identify several novel candidate oncogenes and assess their correlation with oncogenic *ErbB2* (*HER2/neu*). We show that loci containing *Wnt* and *Fgf/Fgfr*-family genes have a significant anti-correlation with the *ErbB2*-transgene, whereas the *Lrfn5* and *Gm26870/Mir101c* loci, but especially the *Eras* locus, are preferentially targeted by MMTV in the *ErbB2*-transgenic mice. The candidate target LRFN5 (leucine-rich repeat and fibronectin type III domain-

containing 5; also known as SALM5, Synaptic Adhesion-Like Molecule 5) is a poorly studied transmembrane adhesion molecule, involved in synapse formation and neurite outgrowth [34, 35]. Of the candidates in the other *ErbB2*-associated MMTV-targeted locus, the long intergenic non-coding RNA *Gm26870* has never been described, to our knowledge, whereas microRNA-101c (*mmu-mir-101c*) has been implicated in cancer before [36]. Although it may be worthwhile to investigate these CISs in the context of HER2+ breast cancer, we focused on *Eras* in this study.

Eras is a unique RAS-family member in various aspects. The gene encodes a constitutively active small GTPase and appears to be exclusively present in mammalian genomes [37]. In mice, *Eras* has been reported to be expressed only in undifferentiated ES cells and teratocarcinomas derived from these cells [21], whereas in human ES cells, *ERAS* expression has not been detected [38]. In mouse ES cells, *Eras* has been shown to activate the PI3K/AKT pathway but not the MAPK/ERK pathway [21], which we also observe in both murine and human mammary cells upon ectopic expression. This is in contrast to the canonical RAS-family members, KRAS, HRAS, and NRAS, which primarily activate the MAPK/ERK pathway instead. *ERAS* is not required for pluripotency of ES cells, but growth rate and tumorigenicity of *ERAS*-null ES cells is significantly reduced, which can be rescued by expression of activated PI3K. This has led to the conclusion that *ERAS*-induced PI3K/AKT-pathway activation is important for the tumor-like growth capacity of ES cells. In accordance, ectopic expression of *Eras* also confers tumorigenic properties to murine embryonic NIH-3T3 fibroblasts [21] and *ERAS* expression has been associated with human gastric cancer [39, 40]. In this study, we show that *Eras* is not expressed during any developmental stage of the adult mouse mammary gland, but that the gene acts as a tumorigenic driver upon ectopic expression in mammary epithelial cells. We specifically demonstrate that *Eras* induces increased cell proliferation and insulin-independent growth.

Importantly, we show that *ERAS* and ERBB2 collaborate to synergistically enhance cell proliferation, anchorage-independent growth in vitro and tumorigenesis in vivo. In human and mouse mammary tumors, ERBB2 is usually present in a heterodimer with ERBB3 [41], in which ERBB2 activates the MAPK/ERK pathway, whereas ERBB3 activates the PI3K/AKT pathway. We show that 42% of *ErbB2*-driven tumors with CIS-associated MMTV insertions no longer express *ErbB3*, in contrast to the spontaneous tumors in non-infected *ErbB2*-transgenic mice, which express *ErbB3* in 100% of the cases, suggesting that the activated MMTV-targets functionally replace ERBB3. Indeed, in its capacity to constitutively activate the PI3K/AKT pathway, the MMTV target *Eras* is able to adopt this role from ERBB3. Correspondingly, tumors expressing

both *ERAS* and *ERBB3* are rare or absent in both the human and murine setting.

Only half of HER2+ breast cancer cases respond to HER2-targeted therapies and this therapy resistance is also reflected in *ErbB2*-transgenic mouse models [42, 43]. Notably, PI3K/AKT-pathway activation is implicated in resistance to the commonly used HER2-targeted therapeutics, Trastuzumab and Lapatinib, specifically through activating mutations in *PIK3CA* (phosphatidylinositol-4,5-bisphosphate 3-kinase, catalytic subunit alpha) or loss of its antagonist *PTEN* (phosphatase and tensin homolog) [31–33, 44–48]. Our data identify *ERAS* as an important gene that hyperactivates the PI3K/AKT pathway and induces resistance to HER2-targeting therapeutics, both in vitro and in vivo. Moreover, we found that *ERAS* mRNA is expressed in at least 13% of HER2+ human breast carcinomas, further subscribing the clinical relevance of *ERAS*. Altogether, these results suggest that *ERAS* expression may be a promising biomarker for de novo therapy resistance. We also demonstrate that *ERAS* may be involved in acquired resistance, as selective pressure by Trastuzumab and Lapatinib leads to upregulation of *ERAS* expression in growing HER2+ breast cancer cells.

The standard treatment for HER2+ breast carcinomas comprises the combination of chemotherapy with Trastuzumab, followed by Lapatinib treatment when tumors do not respond to Trastuzumab. Considering that *ERAS* was recently also implicated in resistance to chemotherapeutic agents in neuroblastoma and gastric cancer cell lines [49, 50], the clinical importance of this gene for therapeutic response is further highlighted. However, large-scale validation of *ERAS* expression as predictive marker for therapy response is hampered by the lack of an *ERAS* probe on the gene expression microarrays used in clinical trials. Promisingly though, we observed in a pre-clinical setting that the combination of suboptimal doses of a PI3-kinase inhibitor with suboptimal doses of Trastuzumab or Lapatinib can abrogate *ERAS*-induced therapy resistance and the oncogenic synergism between *ERAS* and *ERBB2*. This combination therapy may therefore offer an important window of opportunity for treatment of HER2+ breast cancer patients with primary or acquired resistance to HER2-targeting drugs.

Material and methods

Patient samples

Our pathology department provided 86 random human primary breast carcinoma samples and associated clinical parameters from women treated between 2007 and 2011 at the NKI. In addition, the NKI's Core Facility Molecular

Pathology & Biobanking (CFMPB) supplied us with RNA samples of 30 randomly selected tumors from a uniform set of 129 HER2+ primary breast carcinomas, obtained from patients treated between 1989 and 2006 at our institute. All patients individually approved the use of tumor tissue for research purposes via opt-out and specific use for this study was approved by the local Translational Research Board, following positive recommendation of the Medical Ethical Committee.

Insertional mutagenesis screens and tumorigenicity assays

The MMTV-induced insertional mutagenesis screens and insertion site mapping followed the previously reported classical splinkerette PCR method [11] or the “Shear-Splink” method [14]. *MMTV-cNeu* mice (*FVB/N-Tg (MMTVneu)202Mul/J*, MGI ID: 1930204), were originally generated by William Muller [7] and bred at the NKI. Tumorigenicity following subcutaneous injection of 1×10^6 viable cells in both flanks of 4-week-old female *BALB/cABomA-nu/nu* (BALB/c nude) mice ($n = 10$ for each group), bred in our institute, was assessed as previously described [15]. The in vivo Lapatinib-resistance experiment and analysis was performed in 4-week-old female *BALB/cAnNRj-Foxn1tm* mice (Janvier Labs, Le Genest-Saint-Isle, France) ($n = 9$ in each group) as described before [15]. Sample size was chosen based on previous experience in s. c. tumor growth studies [15]. No animals were excluded in these studies, except animals that died prematurely because of causes unrelated to the experiment. All grafted animals within the experiment were culled when the largest tumors reached ~1.5 cm or the animals reached the age of 4 months. The observer was blinded to the type of treatment when measuring tumor size. The “survival” package in the statistical programming language R was used to plot the Kaplan–Meier curves and to calculate log-rank tests. All mouse experiments were approved by the local Animal Experiments Committee (DEC nr 08.061) and strictly followed the Dutch Code of Practice for Research with Laboratory Animals in Cancer Research.

Cell culture, vectors, and in vitro experiments

Details on the sources of the used cell lines, culturing conditions, transduction, in vitro treatments and cell proliferation, apoptosis, dose response, and anchorage-independent growth (soft agar) assays are described before [15]. Constructs containing full-length human and murine *ERAS*-cDNA were a kind gift from Liesbeth Vredeveld (NKI, Amsterdam, The Netherlands). These genes were cloned into pBABE-plasmids with the puromycin resistance gene, using the restriction sites of *Bam*HI and

SalI. pcDNA3-NeuNT construct was kindly provided by Bill Muller (McGill Cancer Center, Montreal, Canada) and the rat *cNeu* (*ErbB2*)-cDNA from this construct was cloned into a pMSCV-plasmid carrying the blasticidin resistance marker, using *HindIII* and *EcoRI* restriction sites. pBABE-vectors containing human RasV12 and KRasV12 were obtained from the labs of Daniel Peeper and René Bernhards (NKI, Amsterdam, The Netherlands), respectively. Empty backbones of these vectors were used as controls.

Expression analysis, Western blotting, and immunohistochemistry

RNA isolation from tissues, tumors, and cell lines, followed by RT-PCR and expression analysis was performed as previously described [15]. Primer sequences are provided in the Supplementary Table 3. Details on lysis and subsequent Western blotting are provided elsewhere [15]. Antibody sources and dilutions used can be found in the Supplementary Table 4. Immunohistochemistry was performed on 4 μ m sections of paraffin-embedded EAF-fixed tumors using a 1:600 diluted polyclonal antibody targeting ERAS (#AP1470; Abgent, San Diego, CA, USA). Before staining the sections were subjected to heat-induced antigen retrieval using a pH 6.1 citrate buffer. The specificity of the antibody is provided by the supplier and was further validated in our own lab (Supplementary Table 4)

Statistical analyses

The number of biological replicates of the tests are provided in the legend of the figures ($n \geq 3$). The statistical programming language R, including the “Bioconductor” and “Survival” packages, were used for statistical analyses. All the statistical tests are specified in the text and/or figure legends. A p -value < 0.05 was considered statistically significant. Distributions and variances of samples (test and control groups) were similar, as determined using R.

Acknowledgements We are grateful to Hugo Horlings and Sabine Linn for support with acquiring clinical samples. We thank William Muller, Joyce Taylor-Papadimitriou, Liesbeth Vredeveld, Katrien Berns, Daniel Peeper, and René Bernhards for sharing materials. We acknowledge graduate students Sarah-Jane Remak and Nina Borràs Agustí for technical assistance.

Compliance with ethical standards

Conflict of interest The authors declare that they have no competing interests.

Open Access This article is licensed under a Creative Commons Attribution-NonCommercial-ShareAlike 4.0 International License, which permits any non-commercial use, sharing, adaptation, distribution and reproduction in any medium or format, as long as

you give appropriate credit to the original author(s) and the source, provide a link to the Creative Commons license, and indicate if changes were made. If you remix, transform, or build upon this article or a part thereof, you must distribute your contributions under the same license as the original. The images or other third party material in this article are included in the article’s Creative Commons license, unless indicated otherwise in a credit line to the material. If material is not included in the article’s Creative Commons license and your intended use is not permitted by statutory regulation or exceeds the permitted use, you will need to obtain permission directly from the copyright holder. To view a copy of this license, visit <http://creativecommons.org/licenses/by-nc-sa/4.0/>.

References

- Engström MJ, Opdahl S, Hagen AI, Romundstad PR, Akslen LA, Haugen OA, et al. Molecular subtypes, histopathological grade and survival in a historic cohort of breast cancer patients. *Breast Cancer Res Treat.* 2013;140:1–11.
- Dawood S, Broglio K, Buzdar AU, Hortobagyi GN, Giordano SH. Prognosis of women with metastatic breast cancer by HER2 status and trastuzumab treatment: an institutional-based review. *J Clin Oncol* 2010;28:92–8.
- Blackwell KL, Burstein HJ, Storniolo AM, Rugo H, Sledge G, Koehler M, et al. Randomized study of lapatinib alone or in combination with trastuzumab in women with ErbB2-positive, trastuzumab-refractory metastatic breast cancer. *J Clin Oncol.* 2010;28:1124–30.
- Gagliato DDM, Jardim DLF, Marchesi MSP, Hortobagyi GN, de Melo Gagliato D, Leonardo Fontes Jardim D, et al. Mechanisms of resistance and sensitivity to anti-HER2 therapies in HER2+ breast cancer. *Oncotarget.* 2016;5:64431–46.
- Muller WJ, Sinn E, Pattengale PK, Wallace R, Leder P, Single-step induction of mammary adenocarcinoma in transgenic mice bearing the activated *c-neu* oncogene. *Cell.* 1988;54:105–15.
- Bouchard L, Lamarre L, Tremblay PJ, Jolicœur P. Stochastic appearance of mammary tumors in transgenic mice carrying the MMTV/*c-neu* oncogene. *Cell.* 1989;57:931–6.
- Guy CT, Webster Ma, Schaller M, Parsons TJ, Cardiff RD, Muller WJ. Expression of the *neu* protooncogene in the mammary epithelium of transgenic mice induces metastatic disease. *Proc Natl Acad Sci Usa* 1992;89:10578–82.
- Andrechek ER, Hardy WR, Siegel PM, Rudnicki MA, Cardiff RD, Muller WJ. Amplification of the *neu/erbB-2* oncogene in a mouse model of mammary tumorigenesis. *Proc Natl Acad Sci USA.* 2000;97:3444–9.
- Rosner A, Miyoshi K, Landesman-Bollag E, Xu X, Seldin DC, Moser AR, et al. Pathway pathology: histological differences between ErbB/Ras and Wnt pathway transgenic mammary tumors. *Am J Pathol.* 2002;161:1087–97.
- Andrechek ER, Laing MA, Girgis-Gabardo AA, Siegel PM, Cardiff RD, Muller WJ. Gene expression profiling of *neu*-induced mammary tumors from transgenic mice reveals genetic and morphological similarities to ErbB2-expressing human breast cancers. *Cancer Res* 2003;63:4920–6.
- Theodorou V, Kimm MA, Boer M, Wessels L, Theelen W, Jonkers J, et al. MMTV insertional mutagenesis identifies genes, gene families and pathways involved in mammary cancer. *Nat Genet* 2007;39:759–69.
- Kim HH, van den Heuvel APJ, Schmidt JW, Ross SR. Novel common integration sites targeted by mouse mammary tumor virus insertion in mammary tumors have oncogenic activity. *PLoS One* 2011;6:e27425.
- Callahan R, Mudunur U, Bargo S, Raafat A, McCurdy D, Boulanger C, et al. Genes affected by mouse mammary tumor virus

- (MMTV) proviral insertions in mouse mammary tumors are deregulated or mutated in primary human mammary tumors. *Oncotarget*. 2012;3:1320–34.
14. Klijn C, Koudijs MJ, Kool J, ten Hoeve J, Boer M, de Moes J, et al. Analysis of tumor heterogeneity and cancer gene networks using deep sequencing of MMTV-induced mouse mammary tumors. *PLoS One* 2013;8:e62113.
 15. Ikink GJ, Boer M, Bakker ERM, Hilkens J. IRS4 induces mammary tumorigenesis and confers resistance to HER2-targeted therapy through constitutive PI3K/AKT-pathway hyperactivation. *Nat Commun*. 2016;7:13567.
 16. Nusse R. Insertional mutagenesis in mouse mammary tumorigenesis. In: Kung H-J, Vogt P, editors. *Retroviral insertion and oncogene activation*. Berlin: Springer; 1991. p. 43–65.
 17. Hilkens J. Recent translational research: oncogene discovery by insertional mutagenesis gets a new boost. *Breast Cancer Res* 2006;8:102.
 18. Callahan R, Smith GH. Common integration sites for MMTV in viral induced mouse mammary tumors. *J Mammary Gland Biol Neoplasia* 2008;13:309–21.
 19. Koudijs MJ, Klijn C, Van Der Weyden L, Kool J, Ten Hoeve J, Sie D, et al. High-throughput semiquantitative analysis of insertional mutations in heterogeneous tumors. *Genome Res* 2011;21:2181–9.
 20. Miyoshi J, Kagimoto M, Soeda E, Sakaki Y. The human c-Ha-ras2 is a processed pseudogene inactivated by numerous base substitutions. *Nucleic Acids Res* 1984;12:1821–8.
 21. Takahashi K, Mitsui K, Yamanaka S, Role of ERas in promoting tumour-like properties in mouse embryonic stem cells. *Nature*. 2003;423:541–5.
 22. Polo JM, Anderssen E, Walsh RM, Schwarz BA, Nefzger CM, Lim SM, et al. A molecular roadmap of reprogramming somatic cells into iPS cells. *Cell*. 2012;151:1617–32.
 23. Yu Y, Liang D, Tian Q, Chen X, Jiang B, Chou BK, et al. Stimulation of somatic cell reprogramming by ERas-Akt-FoxO1 signaling axis. *Stem Cells* 2014;32:349–63.
 24. Zhao Z-A, Yu Y, Ma H-X, Wang X-X, Lu X, Zhai Y, et al. The roles of ERAS during cell lineage specification of mouse early embryonic development. *Open Biol*. 2015; 5: 150092. <https://doi.org/10.1098/rsob.150092>.
 25. Akagi K, Suzuki T, Stephens RM, Jenkins NA, Copeland NG. RTCGD: retroviral tagged cancer gene database. *Nucleic Acids Res* 2004;32:D523–27.
 26. Ikink GJ, Hilkens J, Insulin receptor substrate 4 (IRS4) is a constitutive active oncogenic driver collaborating with HER2 and causing therapeutic resistance. *Mol Cell Oncol*. 2017;4:e1279722.
 27. Holbro T, Beerli RR, Maurer F, Koziczak M, Barbas CF, Hynes NE. The ErbB2/ErbB3 heterodimer functions as an oncogenic unit: ErbB2 requires ErbB3 to drive breast tumor cell proliferation. *Proc Natl Acad Sci Usa* 2003;100:8933–8.
 28. Lee-Hoeflich ST, Crocker L, Yao E, Pham T, Munroe X, Hoeflich KP, et al. A central role for HER3 in HER2-amplified breast cancer: implications for targeted therapy. *Cancer Res* 2008;68:5878–87.
 29. Ciriello G, Gatza ML, Beck AH, Wilkerson MD, Rhie SK, Pastore A, et al. Comprehensive molecular portraits of invasive lobular breast cancer. *Cell*. 2015;163:506–19.
 30. Pereira B, Chin S-F, Rueda OM, Vollan H-KM, Provenzano E, Bardwell HA, et al. The somatic mutation profiles of 2,433 breast cancers refines their genomic and transcriptomic landscapes. *Nat Commun* 2016;7:11479.
 31. Berns K, Horlings HM, Hennessy BT, Madiredjo M, Hijmans EM, Beelen K, et al. A functional genetic approach identifies the PI3K pathway as a major determinant of trastuzumab resistance in breast cancer. *Cancer Cell*. 2007;12:395–402.
 32. Eichhorn PJA, Gili M, Scaltriti M, Serra V, Guzman M, Nijkamp W, et al. Phosphatidylinositol 3-kinase hyperactivation results in lapatinib resistance that is reversed by the mTOR/phosphatidylinositol 3-kinase inhibitor NVP-BEZ235. *Cancer Res* 2008;68:9221–30.
 33. Majewski IJ, Nuciforo P, Mitterpergher L, Bosma AJ, Eidtmann H, Holmes E, et al. PIK3CA mutations are associated with decreased benefit to neoadjuvant human epidermal growth factor receptor 2-targeted therapies in breast cancer. *J Clin Oncol* 2015;33:1334–9.
 34. Wang PY, Seabold GK, Wenthold RJ. Synaptic adhesion-like molecules (SALMs) promote neurite outgrowth. *Mol Cell Neurosci*. 2008;39:83–94.
 35. Mah W, Ko J, Nam J, Han K, Chung WS, Kim E. Selected SALM (synaptic adhesion-like molecule) family proteins regulate synapse formation. *J Neurosci*. 2010;30:5559–68.
 36. Vyazunova I, Maklakova VI, Berman S, De I, Steffen MD, Hong W, et al. Sleeping Beauty Mouse Models Identify Candidate Genes Involved in Gliomagenesis. *PLoS ONE*. 2014;9:e113489..
 37. Colicelli J. Human RAS superfamily proteins and related GTPases. *Sci Stke* 2004;2004:RE13.
 38. Kameda T, Thomson JA. Human ERas gene has an upstream premature polyadenylation signal that results in a truncated, noncoding transcript. *Stem Cells* 2005;23:1535–40.
 39. Kaizaki R, Yashiro M, Shinto O, Yasuda K, Matsuzaki T, Sawada T, et al. Expression of ERas oncogene in gastric carcinoma. *Anticancer Res* 2009;29:2189–93.
 40. Kubota E, Kataoka H, Aoyama M, Mizoshita T, Mori Y, Shimura T, et al. Role of ES cell-expressed Ras (ERas) in tumorigenicity of gastric cancer. *Am J Pathol*. 2010;177:955–63.
 41. Hynes NE, MacDonald G. ErbB receptors and signaling pathways in cancer. *Curr Opin Cell Biol* 2009;21:177–84.
 42. Knutson KL, Almand B, Dang Y, Disis ML. neu Antigen-negative variants can be generated after neu-specific antibody therapy in neu transgenic mice. *Cancer Res* 2004;64:1146–51.
 43. Ellis MJ, Perou CM. The genomic landscape of breast cancer as a therapeutic roadmap. *Cancer Discov* 2013;3:27–34.
 44. Nagata Y, Lan K-H, Zhou X, Tan M, Esteva FJ, Sahin AA, et al. PTEN activation contributes to tumor inhibition by trastuzumab, and loss of PTEN predicts trastuzumab resistance in patients. *Cancer Cell*. 2004;6:117–27.
 45. Esteva FJ, Guo H, Zhang S, Santa-Maria C, Stone S, Lanchbury JS, et al. PTEN, PIK3CA, p-AKT, and p-p70S6K status: association with trastuzumab response and survival in patients with HER2-positive metastatic breast cancer. *Am J Pathol*. 2010;177:1647–56.
 46. Wang L, Zhang Q, Zhang J, Sun S, Guo H, Jia Z, et al. PI3K pathway activation results in low efficacy of both trastuzumab and lapatinib. *BMC Cancer*. 2011;11:248.
 47. Chandarlapaty S, Sakr RA, Giri D, Patil S, Heguy A, Morrow M, et al. Frequent mutational activation of the PI3K-AKT pathway in trastuzumab-resistant breast cancer. *Clin Cancer Res* 2012;18:6784–91.
 48. Hanker AB, Pfeifferle AD, Balko JM, Kuba MG, Young CD, Sánchez V, et al. Mutant PIK3CA accelerates HER2-driven transgenic mammary tumors and induces resistance to combinations of anti-HER2 therapies. *Proc Natl Acad Sci USA*. 2013;110:14372–7.
 49. Aoyama M, Kataoka H, Kubota E, Tada T, Asai K. Resistance to chemotherapeutic agents and promotion of transforming activity mediated by embryonic stem cell-expressed Ras (ERas) signal in neuroblastoma cells. *Int J Oncol* 2010;37:1011–6.
 50. Kubota E, Kataoka H, Tanaka M, Okamoto Y, Ebi M, Hirata Y, et al. ERas enhances resistance to CPT-11 in gastric cancer. *Anticancer Res* 2011;31:3353–60.